



Published in final edited form as:

Nat Struct Mol Biol. 2021 February ; 28(2): 128–131. doi:10.1038/s41594-020-00547-5.

Cold sensitivity of the SARS-CoV-2 spike ectodomain

Robert J Edwards^{1,2,*}, Katayoun Mansouri^{1,‡}, Victoria Stalls^{1,‡}, Kartik Manne^{1,‡}, Brian Watts¹, Rob Parks¹, Katarzyna Janowska¹, Sophie M. C. Gobeil¹, Megan Kopp¹, Dapeng Li¹, Xiaozhi Lu¹, Zekun Mu¹, Margaret Deyton¹, Thomas H Oguin III¹, Jordan Spreng¹, Wilton Williams^{1,2}, Kevin O. Saunders^{1,3}, David Montefiori^{1,3}, Gregory D. Sempowski¹, Rory Henderson^{1,2}, S. Munir Alam^{1,2}, Barton F. Haynes^{1,2,4}, Priyamvada Acharya^{1,3,*}

¹Duke Human Vaccine Institute, Durham NC 27710, USA

²Duke University, Department of Medicine, Durham NC 27710, USA

³Duke University, Department of Surgery, Durham NC 27710, USA

⁴Duke University, Department of Immunology, Durham NC 27710, USA

Abstract

The SARS-CoV-2 spike (S) protein, a primary target for COVID-19 vaccine development, presents its Receptor Binding Domain in two conformations, receptor-accessible “up” or receptor-inaccessible “down” states. Here we report that the commonly used stabilized S ectodomain construct “2P” is sensitive to cold temperature, and this cold sensitivity is abrogated in a “down” state-stabilized ectodomain. Our findings will impact structural, functional and vaccine studies that use SARS-CoV-2 S ectodomain.

The spike (S) protein of SARS-CoV-2 mediates receptor binding and cell entry and is a key target for vaccine development efforts. Stabilized S ectodomain constructs have been developed that mimic the native spike, bind ACE-2 receptor^{1,2}, and present epitopes for neutralizing antibodies on their surface^{3–6}. The so-called “2P” S-ectodomain construct (2P S) comprises residues 1–1208 of SARS-CoV-2 S and contains two proline substitutions in the C-terminal S2 domain, designed to stabilize the pre-fusion S conformation; a C-terminal foldon trimerization motif; and a mutation that abrogates the furin cleavage site¹ (Figure

Users may view, print, copy, and download text and data-mine the content in such documents, for the purposes of academic research, subject always to the full Conditions of use:http://www.nature.com/authors/editorial_policies/license.html#terms

*Correspondence to: Robert J Edwards (rj.edwards@duke.edu) and Priyamvada Acharya (priyamvada.acharya@duke.edu).

‡These authors contributed equally.

Author contributions

R.J.E., K.Mansouri., V.S. and P.A. discovered the effect of storage temperature on spike stability. R.J.E. led NSEM studies and established quantitative metrics for spike QC. K.Mansouri collected NSEM data and performed analyses. V.S. purified proteins and performed thermostability measurements. K.Manne purified proteins, performed SPR assays, prepared samples for NSEM, Tycho, ELISA, SPR and DSC measurements, and coordinated the study between the different research teams. B.W. performed DSC measurements. R.P., M.D. J.S. and W.W. performed ELISA assays. D.L., X.L., K.O.S. and G.S. isolated antibodies from convalescent patient. S.G. and K. J. purified proteins and performed thermostability assays. M.F.K purified proteins. Z.M. performed binding measurements. T.H.O, D.M. and G.S. performed neutralization assays. R.H. initiated the DSC experiments and provided the rS2d, 2P-N234A and 2P-N165A constructs prior to publication. S.M.A. supervised the DSC experiments. B.F.H. supervised ELISA experiments and antibody isolation. P.A. oversaw and led the study, and co-wrote the paper with R.J.E. and V.S. All authors reviewed and commented on the manuscript.

Competing interests

The authors declare no competing interests.

1a). This and similar constructs have been widely used for structural biology and vaccine studies^{1–3,7,8}. Purified S ectodomain proteins⁹ are assessed for quality control by SDS-PAGE, size exclusion chromatography (SEC), differential scanning fluorimetry (DSF)¹⁰, and negative stain electron microscopy (NSEM). The latter has been particularly informative because it reveals the structural integrity of individual molecules, allowing us to examine preparations that look similar by bulk methods such as SDS-PAGE and SEC (Supplementary Figure 1). The observed variability between preparations suggests a fragile S ectodomain, and measures to overcome the issue have been previously reported^{11,12}.

Here we link the apparent fragility of 2P S to its rapid denaturation upon storage at 4 °C (Figure 1b). We followed the structural, biophysical and antigenic properties of 2P S stored under different temperatures conditions (Figure 1, Extended Data Figures 1–2, Supplementary Tables 1–2, Supplementary Figures 2–6). 2P S was produced in 293F cells at 37 °C and purified at room temperature within 6–8 hours (Supplementary Figure 1). We performed NSEM analysis of 2P S incubated at different temperatures (Figure 1b, Extended Data Figure 1d–e). Freshly prepared 2P S samples assessed on the same day they were purified showed on average 75% well-formed spikes, with characteristic kite-shaped morphology on NSEM micrographs and 2D class averages. This fraction slightly decreased to 64% after one cycle of freeze/thaw and to 59% after room temperature (22 °C) storage for 5–7 days, and it was substantially reduced to 5% after storage at 4 °C for 5–7 days. In contrast, after 1-week storage at 37 °C, we observed 83% well-formed spike. Furthermore, well-formed spike could be recovered after storage at 4 °C for a week with a 3-hour incubation at 37 °C to ~75%, and 3D classification of those particles showed the typical populations of all-RBD-down and 1-RBD-up spike that we reported previously for freshly prepared samples⁹ (Supplementary Figure 6). No further recovery from 4 °C storage was observed after longer incubations at 37 °C, which actually led to slight aggregation; Extended Data Figure 1e).

SDS-PAGE analysis of 2P S samples stored at different temperatures did not indicate any appreciable protein degradation, although we did observe an increase in higher molecular weight bands for samples stored at 37 °C for a week (Supplementary Figure 3). Similarly to our NSEM results, we saw substantial differences in the quality and dispersion of particles in cryo-EM grids depending on the storage temperature of the specimen (Supplementary Figure 4).

The S ectodomain was reported to exhibit conformational changes in response to pH¹², so we asked whether the 2P S denaturation we observed was due to temperature-dependent pH changes in the Tris pH 8.0 buffer used¹³. A Tris buffer solution that measures pH 8.0 at 25 °C would measure ~pH 8.6 at 4 °C. We performed SEC purification of a 2P S preparation into MOPS buffer pH 7.4; with smaller temperature dependence compared to Tris¹³, MOPS buffer should change only slightly, to pH 7.42, at 4 °C. Cold-storage at pH 7.42 (MOPS buffer) reduced the spike fraction to 4%, similar to the average of 5% for cold-storage in Tris buffer (Figure 1b). Thus, temperature change appears to be the primary cause of 2P S denaturation, and not the pH shift within this range. We also tested the temperature effect at acidic pH and found that incubating 2P S at 4 °C in MES, pH 6 buffer reduced but did not eliminate the cold sensitivity.

Next, we examined whether the observed cold sensitivity is a property of the bulk protein in solution rather than an artifact of the NSEM sample preparation. First, we used a rapid DSF assay¹⁰ that measures changes in the protein intrinsic fluorescence as a thermal ramp is applied. The changes in fluorescence signal indicate transitions in the folding state of a protein, and the temperature at which a transition occurs is called the inflection temperature (T_i). Distinct profile shifts were observed for 2P S samples stored at different temperatures, with T_i shifted toward lower temperatures for samples stored at 4 °C, indicating lower protein stability, compared to samples stored at 22 °C or 37 °C (Figures 1c and Supplementary Table 1). Next, we measured melting temperatures (T_m) using differential scanning calorimetry (DSC) (Figure 1c, Supplementary Table 1 and Supplementary Figure 5): after one-week storage at 37 °C, the 2P S sample featured an asymmetric unfolding transition with T_m of 65.5 °C. After one-week storage at 22 °C, we observed a second low- T_m transition at 48.2 °C. After one-week storage at 4 °C, we observed a similar two-peak profile with a markedly more pronounced low- T_m transition ($T_m = 48.4$ °C). Upon returning the 4 °C sample to 37 °C for 3 hours prior to analysis, we observed an amplitude reduction of the low- T_m transition ($T_m = 49.2$ °C) and a corresponding amplitude increase in the high- T_m transition ($T_m = 66.0$ °C). Thus, the DSC results confirm that storage at 4 °C destabilizes 2P S compared to samples stored at 22 °C or 37 °C, and that returning the destabilized 2P S to 37 °C for 3 hours substantially restores its stability, although the presence of the low- T_m peak suggests that the recovery is partial.

We next tested the effects of cold-induced instability on ligand binding to 2P S, by SPR and ELISA (Figures 1d and Extended Data Figures 2–3). We found that 2P S stored at 4 °C showed higher binding to antibody CR3022 and to receptor ACE-2, which both require an “up” RBD conformation for stable binding^{1,9,12}, compared to freshly prepared protein. In contrast, cold storage reduced binding to antibody 2G12, which recognizes a quaternary glycan epitope in the S2 subunit¹⁴, indicating loss of quaternary structure during cold storage. We also tested two antibodies isolated from a COVID-19 convalescent donor, with epitopes mapped to the ACE-2 binding site (DH1179) and to the S2 region of spike (DH1189.1) (Extended Data Figure 3, Supplementary Figures 7–8). Both antibodies showed different binding profiles depending on the temperature at which 2P S was stored. We next tested CR3022 and 2G12 binding to a 2P S sample that was flash-frozen in liquid N₂, stored in single-use aliquots at –80 °C and thawed by incubation at 37 °C (Supplementary Figure 9). Freeze-thaw increased CR3022 binding to the 2P S compared to fresh sample, but incubating the thawed sample at 37 °C for 20 min reversed the effect, with binding activity similar to the levels observed with fresh sample.

These results suggested that cold-induced denaturation of spike was associated with increased RBD-exposure of the S ectodomain. We thus asked whether a “down” state stabilized S ectodomain might be resistant to cold-induced denaturation (Figure 2). Here we included a variant that combined the previously described rS2d⁹ and HexaPro mutations¹¹ (Figure 2a). This new variant, named rS2d-HexaPro, showed higher production yields compared to rS2d⁹. Similarly to rS2d⁹, rS2d-Hexapro particles appear 100 % in a 3-RBD-down conformation as seen by NSEM (Figure 2b, Supplementary Figure 10 and Supplementary Video 1). Both HexaPro and rS2d-HexaPro appeared more resistant to cold-induced denaturation than 2P S (Figure 1b), with rS2d-HexaPro showing higher intact spike

percentage than HexaPro (Figure 2b). Thermostability and binding studies (Figures 2c,d) further confirmed that HexaPro and rS2d-HexaPro were more resistant to cold destabilization compared to the 2P version (Figure 1). Two glycan-deleted mutants, 2P-N165A and 2P-N234A¹⁵, which have altered RBD-up propensity, showed substantial reduction of intact spike after incubation at 4 °C (Figure 2f). The rS2d mutations (D985C, S383C) introduce an inter-protomer disulfide bond between the RBD and the S2 domain. Another study confirmed the stabilization effect of this disulfide bond, as well as that of an introduced disulfide bond between residues 987 and 413, for spike stored at 4 °C¹⁶. These data suggest that inter-protomer disulfide linkages may be a general strategy to stabilize the 2P spike ectodomain and preventing its cold-induced denaturation.

Compared to 2P S, rS2d-HexaPro binding to ACE-2 was substantially reduced for samples stored at all temperatures, as expected for a spike fixed in an RBD-down conformation. Similarly, binding to 2G12 remained same for the rS2d-HexaPro construct irrespective of the storage temperature. For HexaPro, binding to ACE-2 was higher and 2G12 binding was reduced with 4 °C -stored protein compared to 37 °C-stored samples, showing that the HexaPro structure remained susceptible to perturbation at lower temperatures, whereas rS2d-HexaPro remains unperturbed upon 4 °C storage.

Overall, our results demonstrate cold sensitivity of the furin-cleavage deficient SARS-CoV-2 ectodomain and highlight the importance of accounting for this effect, in order to obtain consistent results in serology assays or other binding studies using the 2P S or similar constructs. Based on these data, we recommend flash-freezing spike ectodomain samples in single-use aliquots, thawing at 37 °C followed by a brief (~20 min) incubation at 37 °C before use in binding studies.

Online methods

Protein expression and purification

SARS-CoV-2 ectodomain constructs were produced and purified^{1,11} as follows. A gene encoding residues 1–1208 of the SARS-CoV-2 S (GenBank: MN908947) with proline substitutions at residues 986 and 987, a “GSAS” substitution at the furin cleavage site (residues 682–685), a C-terminal T4 fibrin trimerization motif, an HRV3C protease cleavage site, a TwinStrepTag and an 8XHisTag was synthesized and cloned into the mammalian expression vector pαH. Plasmids were transiently transfected into FreeStyle-293F cells using Turbo293 (SpeedBiosystems). Cells were grown in a 37 °C incubator with 9 % CO₂ and 120 rpm rotary motion. Protein was purified on the sixth day post-transfection from filtered supernatant using StrepTactin resin (IBA), followed by SEC purification using a Superose 6 10/300 Increase column in nCoV buffer (2mM Tris, pH 8.0, 200 mM NaCl, 0.02% sodium azide). rS2d-Hexapro was also grown in CHO cells. Plasmids were transiently transfected into CHO cells using ExpiFectamine CHO Transfection Kit (ThermoFisher), and protein was purified on the sixth day post-transfection. All protein purification steps including Strep-tag purification and SEC were performed at room temperature. The spikes were purified the same day that the cells were harvested and the purification was completed within 6–8 hours. The purified protein was flash frozen and

stored at -80°C in single-use aliquots. Each aliquot was thawed and briefly incubated (~ 20 min) at 37°C before use.

Antibodies were produced in Expi293 cells and purified by Protein A affinity. For ACE-2 constructs, the ACE-2 C-terminus was fused with either the human or mouse Fc region including C-terminal 6X His-tag on the Fc domain. ACE-2 with human Fc tag was purified by Protein A affinity chromatography, and ACE-2 with mouse Fc tag was purified by Ni-NTA chromatography.

Negative-stain electron microscopy

Spike samples were incubated for specified times in nCoV buffer at 4, 22 or 37°C , then moved to room temperature to prepare NSEM grids, which was complete in less than 5 min. Samples were diluted to $100\ \mu\text{g}/\text{ml}$ with room-temperature buffer containing 20 mM HEPES pH 7.4, 150 mM NaCl, 5% glycerol and 7.5 mM glutaraldehyde, and incubated 5 min; then glutaraldehyde was quenched for 5 min by addition of 1M Tris stock to a final concentration of 75 mM. A 5- μl drop of sample was applied to a glow-discharged, carbon-coated grid for 10–15 s, blotted, stained with 2% uranyl formate, blotted and air-dried. Images were obtained with a Philips EM420 electron microscope at 120 kV, 82,000 \times magnification, and a 4.02 \AA pixel size. The RELION program¹⁷ was used for particle picking, 2D and 3D class averaging.

Thermostability assays

Thermostability of the S ectodomain samples was measured using DSF and DSC. Samples were purified and buffer exchanged into HBS buffer (10 mM HEPES, 150 mM NaCl, pH 7.4) by SEC on a Superose 6 10/300 column. DSF assay was performed using Tycho NT. 6 (NanoTemper Technologies). Spike variants were diluted (0.15 mg/ml) in HBS and run in triplicate. Intrinsic fluorescence was recorded at 330 nm and 350 nm while heating the sample from 35–95 $^{\circ}\text{C}$ at a rate of 30 $^{\circ}\text{C}/\text{min}$. The ratio of fluorescence (350/330 nm) and inflection temperatures (T_i) were calculated by Tycho NT. 6.

DSC measurements were performed using the NanoDSC platform (TA instruments; New Castle, DE). Samples that had been incubated at 22 $^{\circ}\text{C}$ or 37 $^{\circ}\text{C}$ were purified by SEC at room temperature and the sample incubated at 4 $^{\circ}\text{C}$ was purified by SEC at 4 $^{\circ}\text{C}$ (Extended Data Figure 2), diluted to 0.2–0.3 mg/mL in HBS, and degassed for 15 min at room temperature prior to analysis. DSC measurements were performed immediately after SEC purification of the samples. DSC cells were conditioned with filtered, degassed HBS prior to sample loading. Protein samples were heated from 10 $^{\circ}\text{C}$ to 100 $^{\circ}\text{C}$ at 1 $^{\circ}\text{C}/\text{min}$ under 3 atm pressure using HBS as the reference buffer. The observed denaturation profiles were buffer subtracted, converted to molar heat capacity, baseline-corrected with a 6th-order polynomial, and fit with 2–4 Gaussian transition models, as needed, using the NanoAnalyze software (TA Instruments). The peak transition temperature (T_m) is reported as the temperature at the maximum observed heat capacity of each transition peak.

Isolation of antibodies from COVID-19 convalescent donors

Human SARS-CoV-2 spike antibodies DH1179 and DH1189.1 were isolated from a COVID-19 convalescent individual. Peripheral blood was collected following informed consent on a Duke University Medical Center approved Institutional Review Board protocol. Briefly, PBMC samples collected after the onset of the symptoms were stained and the memory B cells were sorted with SARS-CoV-2 Spike-2P probes. Antibody IgH and IgK/L genes were recovered from the single-cell sorted cells, cloned into human IgG1 constant region backbone, and purified by Protein A beads as previously described¹⁸.

ELISA assays

Spike samples were pre-incubated at different temperatures then tested for antibody- or ACE-2-binding in ELISA assays as previously described^{19,20}. Assays were run in two formats. In the first format antibodies or ACE-2 protein were coated on 384-well plates at 2 µg/ml overnight at 4 °C, washed, blocked and followed by two-fold serially diluted spike protein starting at 25 µg/ml. Binding was detected with polyclonal anti-SARS-CoV-2 spike rabbit serum (developed in our lab), followed by goat anti-rabbit-HRP (Abcam #ab97080) and TMB substrate (Sera Care Life Sciences #5120-0083). Absorbance was read at 450 nm. In the second format, serially diluted spike protein was bound in individual wells of 384-well plates, which were previously coated with streptavidin (Thermo Fisher Scientific #S-888) at 2 µg/ml and blocked. Proteins were incubated at room temperature for 1 hour, washed, then human mAbs were added at 10 µg/ml. Antibodies were incubated at room temperature for 1 hour, washed and binding detected with goat anti-human-HRP (Jackson ImmunoResearch Laboratories, #109-035-098) and TMB substrate.

Commercially obtained constructs of SARS-CoV-2 spike ectodomain (S1+S2 ECD, S2 ECD and RBD) (Sino Biological Inc cat# 40589-V08B1 and 40590-V08B respectively and RBD from Genescript cat# Z03483) were coated directly on 384-well plates at 2 µg/ml and incubated overnight at 4 °C. Plates were washed, blocked and human mAbs three-fold serially diluted from 100 µg/ml were added for 1 hour at room temp followed by washing. Binding was detected with goat anti-human IgG-HRP followed by TMB substrate.

Microneutralization assay

Live SARS-CoV-2 Microneutralization (MN) assays were adapted from Berry et al.²¹ In short, sera or purified antibodies are diluted two-fold and incubated with 100 TCID₅₀ virus for 1 hour. These dilutions are used as the input material for a TCID₅₀. Each batch of MN includes known neutralizing and non-neutralizing controls. Data are reported as the last concentration at which a test sample protects Vero E6 cells. Recently, a fluorescent infectious clone of SARS-CoV-2 was developed²².

Plaque Reduction Neutralization Test (PRNT)

Live SARS-CoV-2 Plaque Reduction Neutralization Test (PRNT) was performed in an assay adapted from Berry et al.²¹ Briefly, two-fold dilutions of a test sample (serum, plasma, purified Ab) are incubated with 50 PFU SARS-CoV-2 for 1 hour (NR-52281; BEI Resources). The antibody/virus mixture was then used to inoculate Vero E6 cells (ATCC). Cultures were then incubated at 37°C, 5% CO₂ for one hour. At the end of the incubation, 1

mL of a viscous overlay (1:1 2X DMEM and 1.2% methylcellulose) was added to each well. Plates were incubated for 4 days. After fixation, staining and washing, plates were dried and plaques counted. Known neutralizing and non-neutralizing antibodies/sera are included in this assay as positive and negative controls, respectively. Plaques from each dilution of each sample are counted and data are reported as the concentration at which 50% of input virus is neutralized.

Pseudovirus Neutralization Assay

SARS-CoV-2 neutralization was assessed with Spike-pseudotyped viruses in 293T/ACE2 cells as a function of reductions in luciferase (Luc) reporter activity. 293T/ACE2 cells were kindly provided by Drs. Mike Farzan and Huihui Mu at Scripps. Cells were maintained in DMEM containing 10% FBS and 3 $\mu\text{g/ml}$ puromycin. An expression plasmid encoding codon-optimized full-length spike of the Wuhan-1 strain (VRC7480), was provided by Drs. Barney Graham and Kizzmekia Corbett at the Vaccine Research Center, National Institutes of Health (USA). The D614G amino acid change was introduced into VRC7480 by site-directed mutagenesis using the QuikChange Lightning Site-Directed Mutagenesis Kit from Agilent Technologies (Catalog # 210518). The mutation was confirmed by full-length spike gene sequencing. Pseudovirions were produced in HEK 293T/17 cells (ATCC cat. no. CRL-11268) by transfection using Fugene 6 (Promega Cat#E2692) and a combination of spike plasmid, lentiviral backbone plasmid (pCMV R8.2) and firefly Luc reporter gene plasmid (pHR' CMV Luc)²³ in a 1:17:17 ratio. Transfections were allowed to proceed for 16–20 hours at 37°C. Medium was removed, monolayers rinsed with growth medium, and 15 ml of fresh growth medium added. Pseudovirus-containing culture medium was collected after an additional 2 days of incubation and was clarified of cells by low-speed centrifugation and 0.45 μm micron filtration and stored in aliquots at -80°C . TCID₅₀ assays were performed on thawed aliquots to determine the infectious dose for neutralization assays (RLU 500–1000x background, background usually averages 50–100 RLU).

For neutralization, a pre-titrated dose of virus was incubated with 8 serial 3-fold or 5-fold dilutions of serum samples or mAbs in duplicate in a total volume of 150 μl for 1 hr at 37 °C in 96-well flat-bottom poly-L-lysine-coated culture plates (Corning Biocoat). Cells were suspended using TrypLE express enzyme solution (Thermo Fisher Scientific) and immediately added to all wells (10,000 cells in 100 μL of growth medium per well). One set of 8 control wells received cells + virus (virus control) and another set of 8 wells received cells only (background control). After 66–72 hrs of incubation, medium was removed by gentle aspiration and 30 μL of Promega 1X lysis buffer was added to all wells. After a 10-minute incubation at room temperature, 100 μL of Bright-Glo luciferase reagent was added to all wells. After 1–2 minutes, 110 μL of the cell lysate was transferred to a black/white plate (Perkin-Elmer). Luminescence was measured using a PerkinElmer Life Sciences, Model Victor2 luminometer. Neutralization titers are the serum dilution (ID50/ID80) or mAb concentration (IC50/IC80) at which relative luminescence units (RLU) were reduced by 50% and 80% compared to virus control wells after subtraction of background RLUs. Maximum percent inhibition (MPI) is the % neutralization at the lowest serum dilution or highest mAb concentration tested. Serum samples were heat-inactivated for 30 minutes at 56 °C prior to assay.

Surface Plasmon Resonance

Antibody binding to SARS-CoV-2 spike constructs was assessed by surface plasmon resonance on a Biacore T-200 (GE-Healthcare) with HBS buffer with 3 mM EDTA and 0.05% surfactant P-20 added. For the data presented in Figure 1d and Extended Data Figures 2 and 3, spike samples that were incubated at 4 °C, 22 °C and 37 °C for a week, were held in the sample chamber at 8 °C, 22 °C and 37 °C, respectively, during the SPR run. The flow cell was maintained at 25 °C, thus all binding assays were performed at 25 °C. Antibodies captured on a CM5 chip coated with amine-coupled human Anti-Fc (8000RU) were assayed by SARS-CoV-2 spike at 200 nM. The surface was regenerated between injections with 3 M MgCl₂ solution for 10 s at 100 µl/min. Sensorgram data were analyzed using the BiaEvaluation software (GE Healthcare).

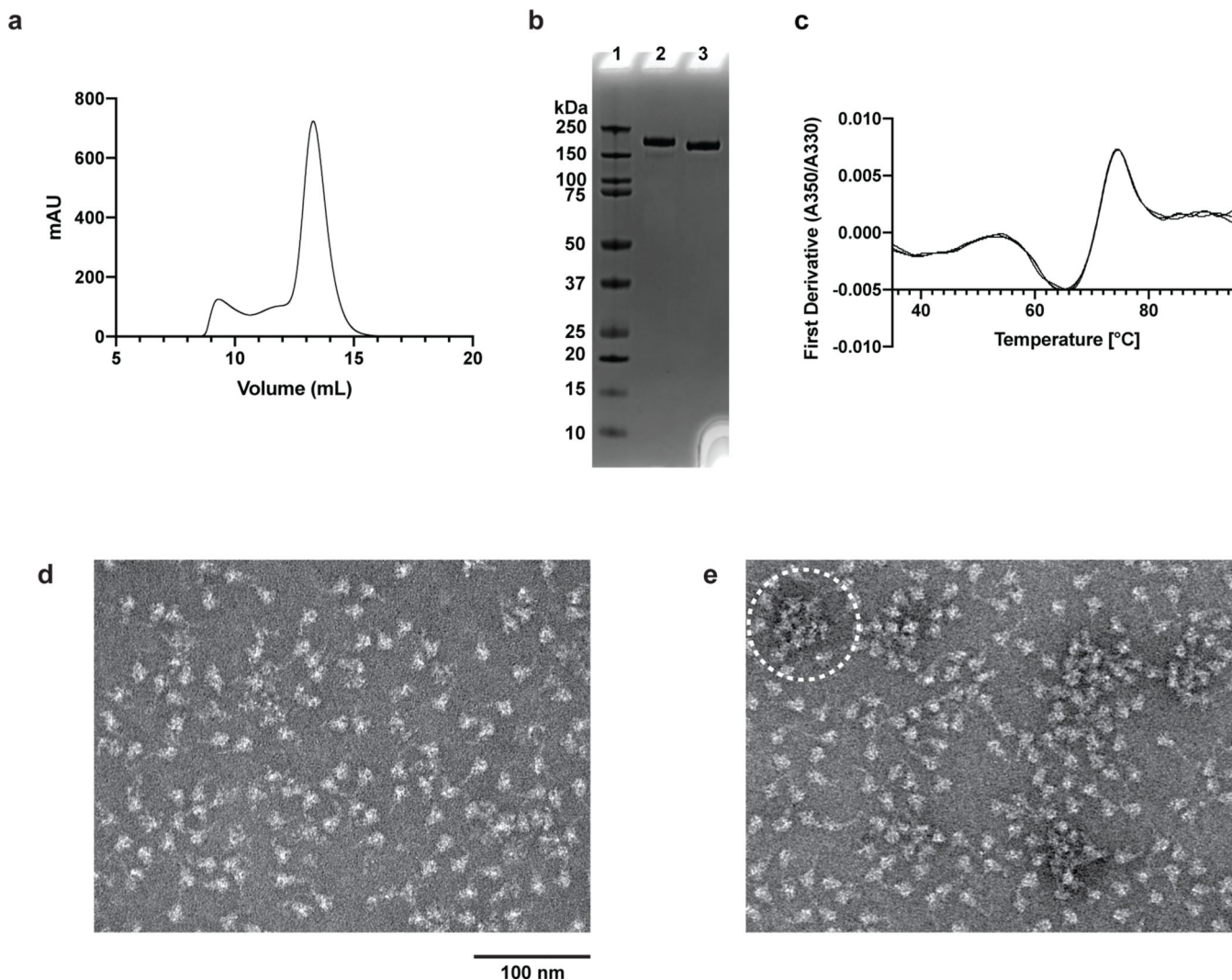
Cryo-EM

Purified SARS-CoV-2 spike preparations were diluted to a concentration of ~1 mg/mL in 2 mM Tris pH 8.0, 200 mM NaCl and 0.02% NaN₃. A 2.5-µL drop of protein was deposited on a CF-1.2/1.3 grid that had been glow discharged for 30 seconds in a PELCO easiGlow™ Glow Discharge Cleaning System. After a 30 s incubation in >95% humidity, excess protein was blotted away for 2.5 seconds before being plunge frozen into liquid ethane using a Leica EM GP2 plunge freezer (Leica Microsystems). Frozen grids were imaged in a Titan Krios (Thermo Fisher) equipped with a K3 detector (Gatan).

Further information on experimental design is available in the Nature Research Reporting Summary linked to this article

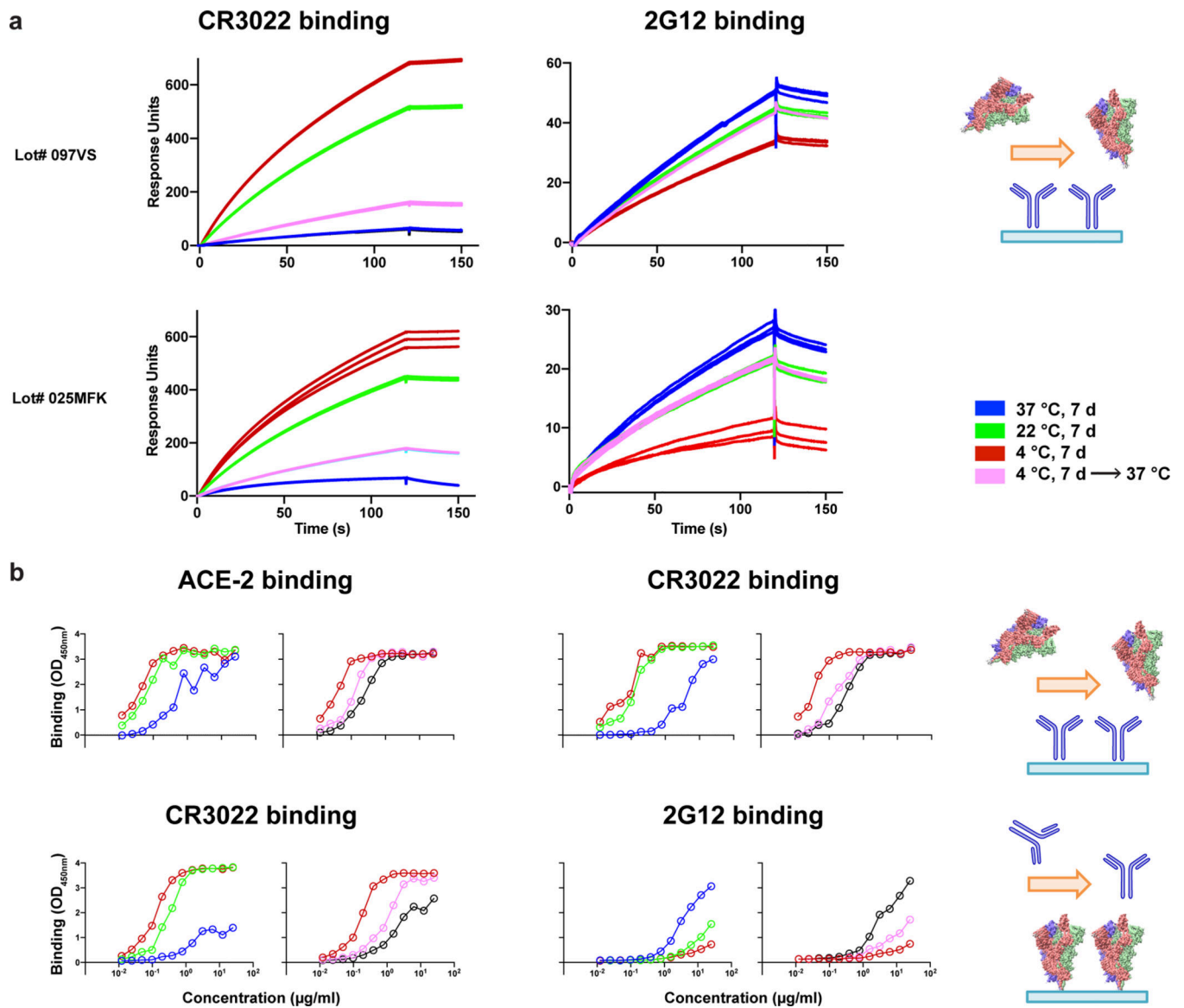
Data Availability—The NSEM reconstruction for rS2d-HexaPro has been deposited in the Electron Microscopy Data Bank with accession code EMD-22934. NSEM reconstructions for the 2P spike after 1-week cold storage followed by 3-hour recovery at 37 °C are deposited with accession codes EMD-22967 and EMD-22968 for the 3-RBD-down and 1-RBD-up states, respectively.

Extended Data



Extended Data Fig. 1. SDS-PAGE and NSEM analysis of SARS-CoV-2 2PS ectodomain incubated at different temperatures.

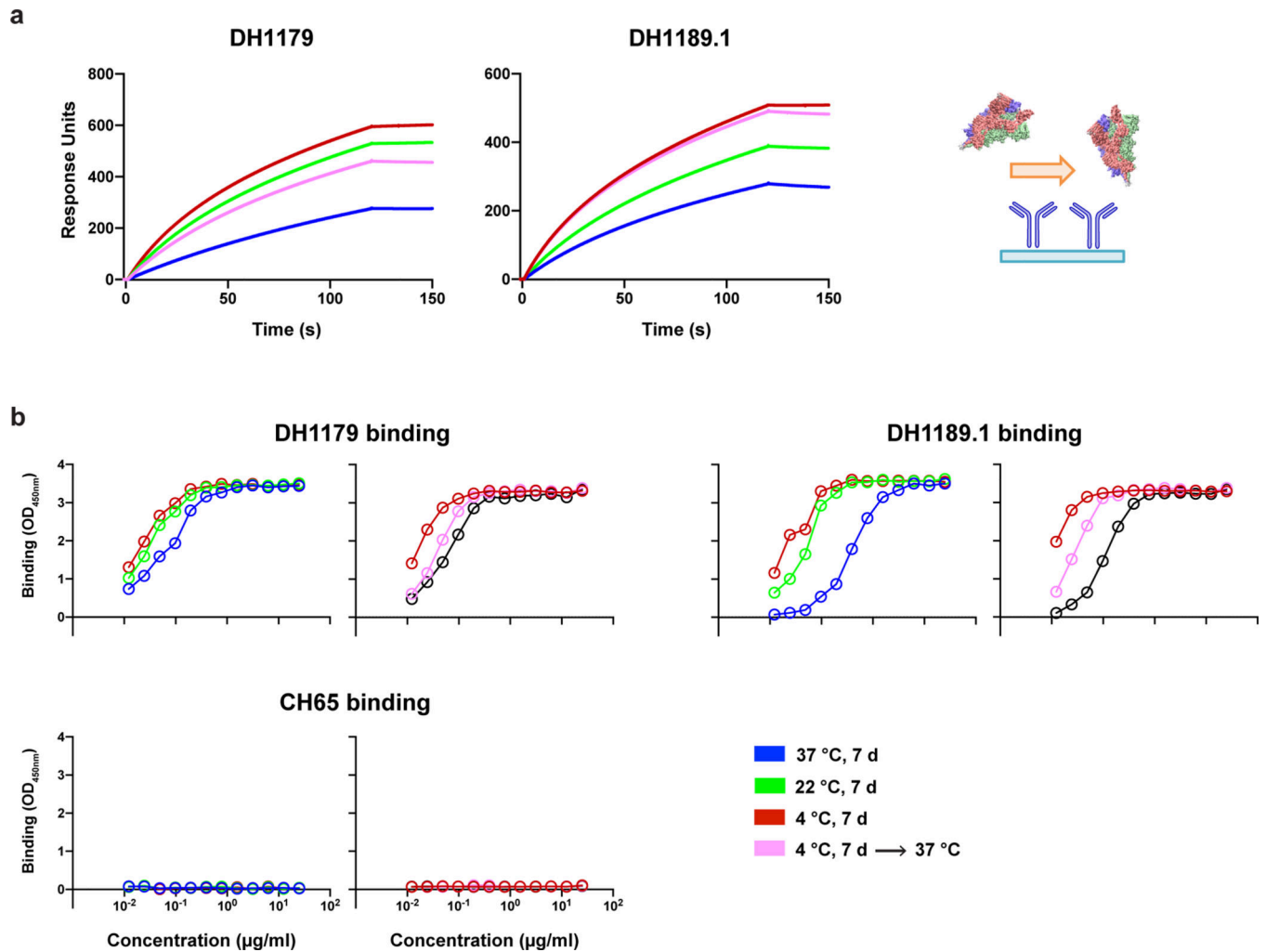
(a) SEC profile, (b) SDS-PAGE analysis (lane 1= molecular weight marker, lane 2= reducing conditions, lane 3= non-reducing conditions) and (c) DSF profile of a freshly purified sample of the 2P spike. (d) NSEM micrograph of 2P spike after storage at 22 °C for one week. (e) NSEM micrograph of 2P spike after storage at 4 °C for one week followed by recovery at 37 °C for 6 days. The circle indicates spike aggregation visible in the micrograph.



Extended Data Fig. 2. Changes in antigenicity of SARS-CoV-2 2PS ectodomain incubated at different temperatures.

(a) Antibody CR3022 IgG (left) and 2G12 IgG (right) binding to two independently purified lots of 2P spike stored at different temperatures measured by SPR. Data for spike samples measured after a 1-week incubation at 37, 22, and 4 °C, are shown in blue, green, and red respectively; sample stored 1 week at 4 °C and then incubated for 6 hours at 37 °C shown in cyan. During the SPR run the sample chamber was maintained at temperatures of 37 °C, 22 °C and 8 °C, for the 37 °C, 22 °C and 4 °C incubated samples, respectively. The binding experiments were carried out at 25 °C. The bar graphs in Fig. 1d show data from Lot # 025MFK. The schematics shows the assay format. (b) ELISA binding profiles showing binding of ACE-2 receptor ectodomain, RBD-directed antibody CR3022, and S2-directed, glycan-reactive antibody, 2G12. The same color scheme was used as for the SPR experiment. The black line indicates a freshly purified 2P spike sample that was flash frozen, then thawed and incubated for 20 min at 37 °C. The schematics show the ELISA format.

The measurements in the top row were done in a format where antibody was coated on the plate and the measurements in the bottom row were done in a format where spike was captured on a strep-coated plate (see Methods).



Extended Data Fig. 3. Antigenic response of SARS-CoV-2 2PS ectodomain incubated at different temperatures to antibodies elicited from convalescent patient sera.

(a) SPR binding profiles showing binding of (left) RBD-directed antibody, DH1179 and (right) S2-directed antibody, DH1189.1 to spike samples incubated for 1 week at either 37 °C (blue), 22 °C (green) or 4 °C (red). Binding to spike sample first incubated at 4 °C for 1 week, then moved to 37 °C for 3 hours prior to the experiment is shown in cyan. (b) ELISA binding profiles showing binding of RBD-directed antibody, DH1179, S2-directed antibody, DH1189.1, and influenza HA-directed antibody CH65 (control) to spike samples incubated at different temperatures (same color scheme as in panel a). The black line indicates a freshly purified 2P spike sample that was flash-frozen, then thawed and incubated for 20 min at 37 °C.

Supplementary Material

Refer to Web version on PubMed Central for supplementary material.

Acknowledgements

This work was supported by NIH NIAID extramural project grants R01 AI145687 (P.A.), AI058607 (G.S.), funding from the Department of Defense HR0011-17-2-0069 (G.S.) and a contract from the State of North Carolina Pandemic Recovery Office through funds from the Coronavirus Aid, Relief, and Economic Security (CARES) Act (B.F.H.). This work utilized the DSC platform supported by the Duke Consortia for HIV/AIDS Vaccine Development (CHAVD) and the Titan Krios microscope in the Duke University Shared Materials Instrumentation Facility (SMIF), a member of the North Carolina Research Triangle Nanotechnology Network (RTNN), which is supported by the National Science Foundation (award number ECCS-2025064) as part of the National Nanotechnology Coordinated Infrastructure (NNCI). The following reagent was deposited by the Centers for Disease Control and Prevention and obtained through BEI Resources, NIAID, NIH: SARS-Related Coronavirus 2, Isolate USA-WA1/2020, NR-52281. MN and PRNT assays were performed in the Virology Unit of the Duke Regional Biocontainment Laboratory, which received partial support for construction from the National Institutes of Health, National Institute of Allergy and Infectious Diseases (UC6-AI058607).

References

1. Wrapp D. et al. Cryo-EM structure of the 2019-nCoV spike in the prefusion conformation. *Science* 367, 1260–1263, doi:10.1126/science.abb2507 (2020). [PubMed: 32075877]
2. Walls AC et al. Structure, Function, and Antigenicity of the SARS-CoV-2 Spike Glycoprotein. *Cell* 181, 281–292 e286, doi:10.1016/j.cell.2020.02.058 (2020). [PubMed: 32155444]
3. Barnes CO et al. Structures of human antibodies bound to SARS-CoV-2 spike reveal common epitopes and recurrent features of antibodies. *bioRxiv*, doi:10.1101/2020.05.28.121533 (2020).
4. Pinto D. et al. Cross-neutralization of SARS-CoV-2 by a human monoclonal SARS-CoV antibody. *Nature*, doi:10.1038/s41586-020-2349-y (2020).
5. Mire CE et al. A Cross-Reactive Humanized Monoclonal Antibody Targeting Fusion Glycoprotein Function Protects Ferrets Against Lethal Nipah Virus and Hendra Virus Infection. *J Infect Dis* 221, S471–S479, doi:10.1093/infdis/jiz515 (2020). [PubMed: 31686101]
6. Ke Z, Oton J; Qu K; Cortese M; Zila V; McKeane L; Nakane T; Zivanov J; Neufeldt CJ; Lu JM; Peukes J; Xiong X; Krausslich HG; Scheres SHW; Bartenschlager R; Briggs JAG Structures, conformations and distributions of SARS-CoV-2 spike protein trimers on intact virions. *bioRxiv* (2020).
7. Liu L. et al. Potent Neutralizing Monoclonal Antibodies Directed to Multiple Epitopes on the SARS-CoV-2 Spike. *bioRxiv*, doi:10.1101/2020.06.17.153486 (2020).
8. Zhou T. et al. Structure-Based Design with Tag-Based Purification and In-Process Biotinylation Enable Streamlined Development of SARS-CoV-2 Spike Molecular Probes. *bioRxiv*, doi:10.1101/2020.06.22.166033 (2020).
9. Henderson R. et al. Controlling the SARS-CoV-2 spike glycoprotein conformation. *Nat Struct Mol Biol*, doi:10.1038/s41594-020-0479-4 (2020).
10. Magnusson AO et al. nanoDSF as screening tool for enzyme libraries and biotechnology development. *FEBS J* 286, 184–204, doi:10.1111/febs.14696 (2019). [PubMed: 30414312]
11. Hsieh CL et al. Structure-based design of prefusion-stabilized SARS-CoV-2 spikes. *Science*, doi:10.1126/science.abd0826 (2020).
12. Zhou T. et al. A pH-dependent switch mediates conformational masking of SARS-CoV-2 spike. *bioRxiv*, doi:10.1101/2020.07.04.187989 (2020).
13. Good NE et al. Hydrogen ion buffers for biological research. *Biochemistry* 5, 467–477, doi:10.1021/bi00866a011 (1966). [PubMed: 5942950]
14. Acharya P. et al. A glycan cluster on the SARS-CoV-2 spike ectodomain is recognized by Fab-dimerized glycan-reactive antibodies. *bioRxiv*, doi:10.1101/2020.06.30.178897 (2020).
15. Henderson R. et al. Glycans on the SARS-CoV-2 Spike Control the Receptor Binding Domain Conformation. *bioRxiv*, doi:10.1101/2020.06.26.173765 (2020).

16. Xiong X. et al. A thermostable, closed SARS-CoV-2 spike protein trimer. *Nat Struct Mol Biol*, doi:10.1038/s41594-020-0478-5 (2020).

Methods-only references

17. Scheres SHW in *Methods in Enzymology Vol. 579* (ed Crowther RA) 125–157 (Academic Press, 2016). [PubMed: 27572726]
18. Liao HX et al. Co-evolution of a broadly neutralizing HIV-1 antibody and founder virus. *Nature* 496, 469–476, doi:10.1038/nature12053 (2013). [PubMed: 23552890]
19. Alam SM et al. Mimicry of an HIV broadly neutralizing antibody epitope with a synthetic glycopeptide. *Science translational medicine* 9, doi:10.1126/scitranslmed.aai7521 (2017).
20. Bonsignori M. et al. Staged induction of HIV-1 glycan-dependent broadly neutralizing antibodies. *Science translational medicine* 9, doi:10.1126/scitranslmed.aai7514 (2017).
21. Berry JD et al. Development and characterisation of neutralising monoclonal antibody to the SARS-coronavirus. *J Virol Methods* 120, 87–96, doi:10.1016/j.jviromet.2004.04.009 (2004). [PubMed: 15234813]
22. Xie X. et al. An Infectious cDNA Clone of SARS-CoV-2. *Cell Host Microbe* 27, 841–848 e843, doi:10.1016/j.chom.2020.04.004 (2020). [PubMed: 32289263]
23. Naldini L. et al. In vivo gene delivery and stable transduction of nondividing cells by a lentiviral vector. *Science* 272, 263–267, doi:10.1126/science.272.5259.263 (1996). [PubMed: 8602510]

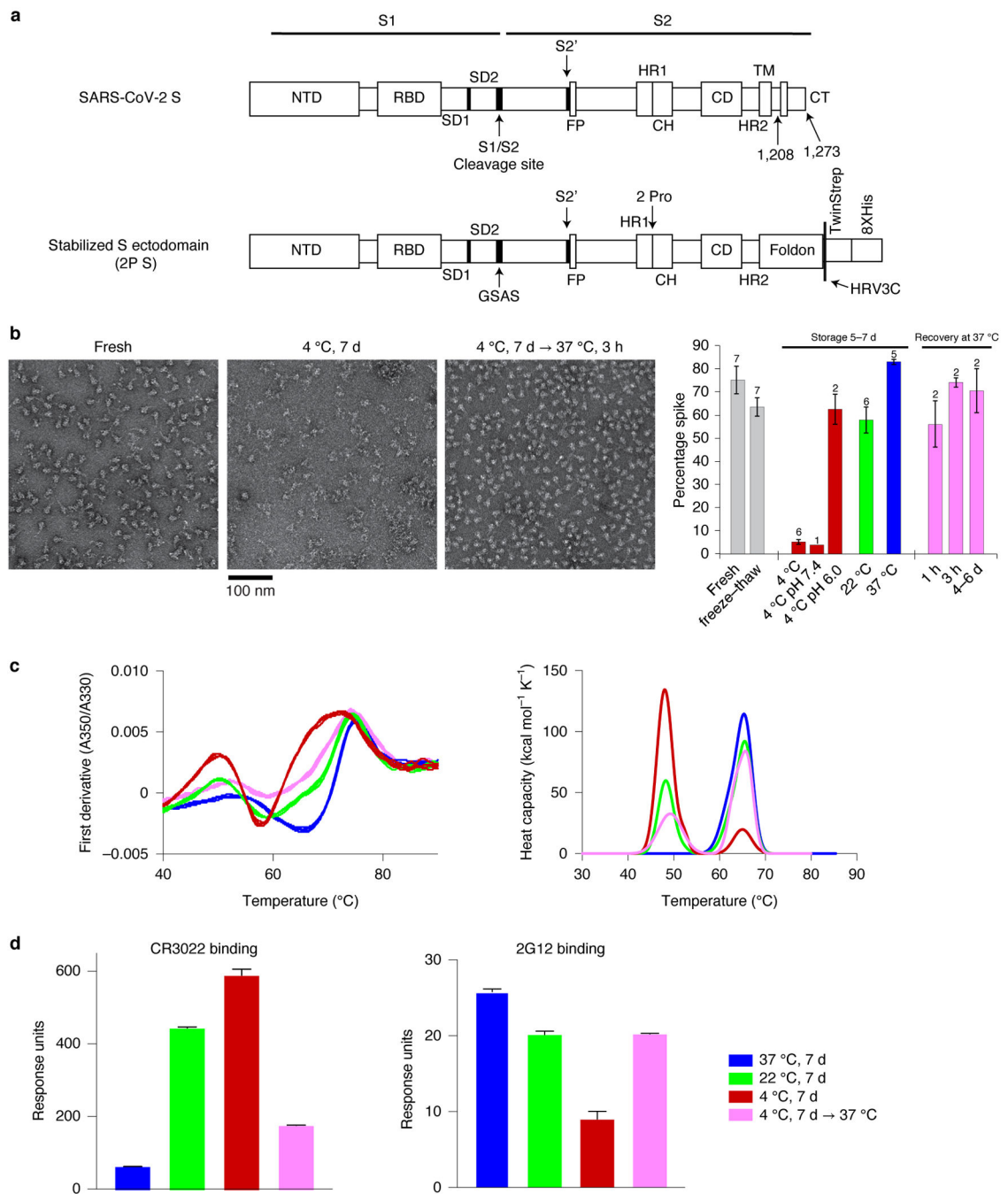


Figure 1. Temperature-dependence of the SARS-CoV-2 S ectodomain. (a) Schematic of the SARS-CoV-2 spike (top, S) and a stabilized, furin cleavage-deficient, soluble ectodomain construct (bottom, 2P). (b) Representative NSEM micrographs of 2P S samples: freshly prepared (left), after storage at 4 °C for 7 days (middle), or stored at 4 °C for 7 days followed by a 3-hour incubation at 37 °C (right). Bar graph summarizes results from NSEM analyses of 2P S samples stored under different conditions. Data shown are mean and range (for N=2) or mean and s.e.m. (from N = 3–7) independent experiments with different protein lots; exact N

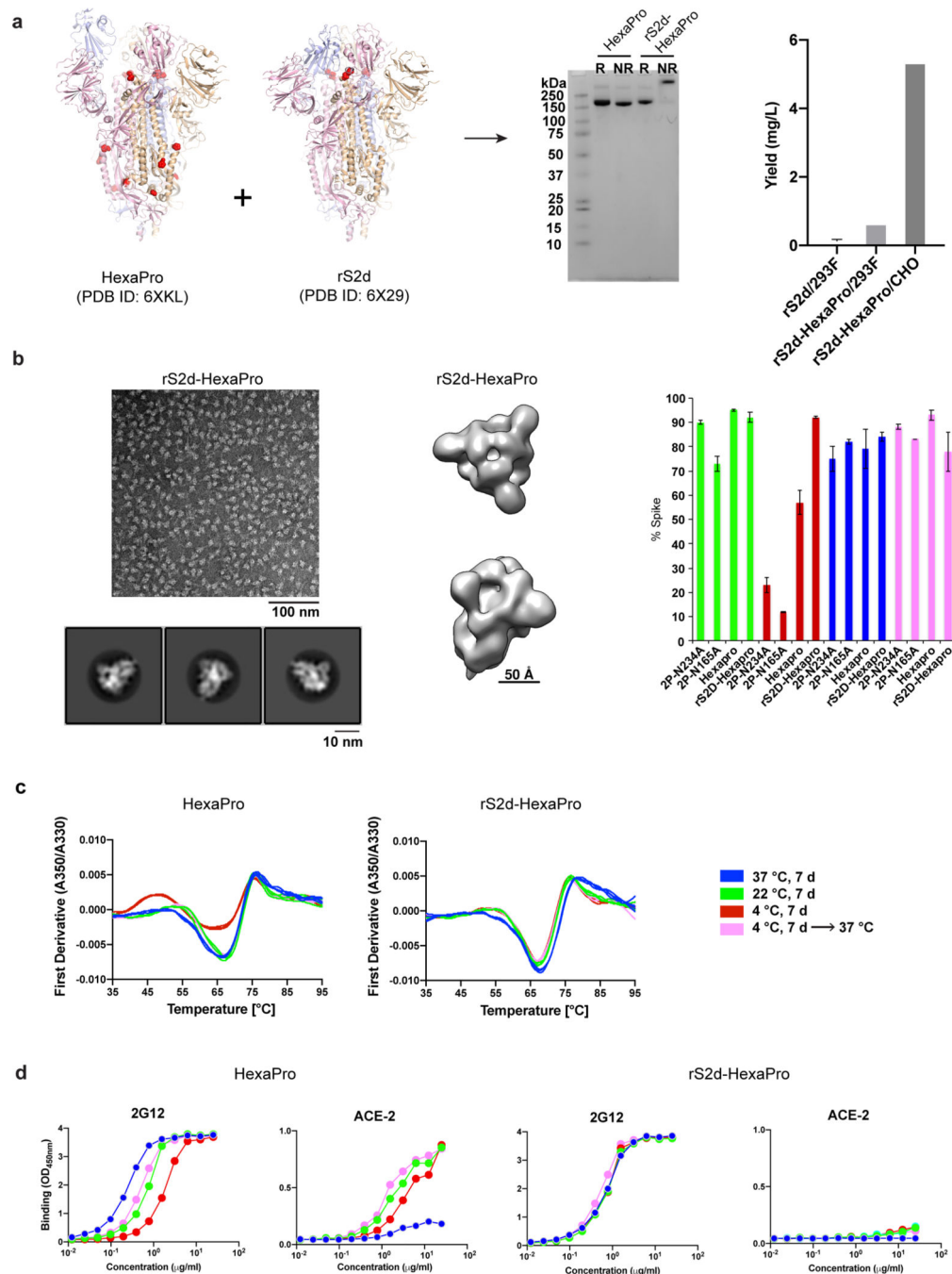
at the top of each bar. (c) Left, DSF profiles following changes in protein intrinsic fluorescence (expressed as ratio between fluorescence at 350 nm and 330 nm) upon applying a thermal ramp. Maxima and minima indicate inflection temperatures, T_i . For each storage condition (color coded as shown in 1d), 5 overlaid curves (technical replicates) are shown. Right. DSC profiles, shown as 2 overlaid curves of technical replicates. (d) Antibody binding to 2P S stored at different temperatures, measured by SPR; antibodies were CR3022 IgG (left) and 2G12 IgG (right). During the SPR run, the sample chamber was maintained at 37 °C, 22 °C or 8 °C, for samples that had been stored at 37 °C, 22 °C or 4 °C, respectively. The binding experiments were carried out at 25 °C. Data are mean and s.e.m. of three technical replicates, and are representative of at least 5 independent experiments, using separate protein lots (two independent repeats are shown in Extended Data Figure 2).

Author Manuscript

Author Manuscript

Author Manuscript

Author Manuscript

**Figure 2.**

Engineered SARS-CoV-2 spike variant, rS2d-HexaPro, is resistant to temperature-dependent structural changes. (a) Left, structures of HexaPro showing a 1-RBD-up conformation (PDB 6XKL) and rS2d (PDB 6X29) showing an all-RBD-down conformation. Middle, SDS-PAGE analysis of HexaPro and rS2d-HexaPro samples, under reducing (R) or non-reducing (NR) conditions. Right, bar graph showing protein yields for rS2d and rS2d-HexaPro produced in 293F or CHO cells. (b) Left, representative NSEM micrograph from a preparation of rS2d-HexaPro (top) and 2D class averages (bottom). Middle, 3D reconstruction of rS2d-HexaPro. (c) Thermal stability analysis showing the first derivative of absorbance (A350/A330) vs. temperature (°C) for HexaPro and rS2d-HexaPro at 37°C, 22°C, and 4°C for 7 days. (d) Binding assays for 2G12 and ACE-2 to HexaPro and rS2d-HexaPro, showing binding (OD_{600nm}) vs. concentration (µg/ml).

Right, bar graph summarizing results from NSEM on S ectodomain variants stored at different temperatures. Data are mean and range (for N=2) or s.e.m. (for N = 3) for independent experiments with different protein lots; exact N indicated at the top of each bar. (c) DSF profiles for Hexapro (left) and rS2d-Hexapro (right). For each storage condition, 3–4 overlaid curves (technical replicates) are shown. (d) Binding of 2G12 and ACE-2 to Hexapro (left) and rS2d-Hexapro (right) measured by ELISA.

Author Manuscript

Author Manuscript

Author Manuscript

Author Manuscript